Supporting Information For

Diversion of Catalytic C-N Bond Formation to Catalytic Oxidation of NH_3 Through Modification of the Hydrogen Atom Abstractor

Peter L. Dunn,† Samantha I. Johnson,† Werner Kaminsky‡ and R. Morris Bullock†

† Center for Molecular Electrocatalysis, Pacific Northwest National Laboratory, P.O. Box 999, Richland, WA 99352, USA

‡ Department of Chemistry, University of Washington, Box 351700, Seattle, Washington 98195-1700, USA

TABLE OF CONTENTS:

Experimental

General Considerations: All manipulations were performed using either standard glovebox or Schlenk techniques. All glassware was oven dried. Benzene-d_6 (99.8% D) and $^{15}NH_3$ (98% purity) were purchased from Cambridge Isotope Laboratories, Inc. The ammonia was used as received. Benzene-d_6 was dried over NaK alloy and vacuum transferred. NH_3 was purchased from Matheson and used as received. Triphenylmethanol and 2,6-di-*tert*-butyl phenol were purchased from Aldrich and used as received. H_2(TMP) was purchased from Frontier Scientific and used as received. (TMP)Ru(CO),[1] tri-*tert*-butyl phenoxyl radical,[2] and 2,6-di-*tert*-butyl-4-tritylphenol[3] were synthesized according to literature procedures.

All solvents used were purified by passage through a neutral alumina column using an Innovative Technology, Inc., PureSolv^{TM} solvent purification system, and stored over activated molecule sieves. NMR spectra were acquired using an INOVA 500 MHz spectrometer. ^{1}H and ^{13}C NMR chemical shifts are reported relative to C_6D_6 (^{1}H: δ 7.16 and ^{13}C: δ 128.06). ^{15}N NMR chemical shift were referenced to an external $CH_3{}^{15}NO_2$ standard (δ 0.00). NMR spectra were processed using MNova 10.0.

Electrochemical experiments were conducted under N_2 at 295 ± 3 K using a standard three-electrode setup, consisting of a 1 mm PEEK-encased glassy carbon working electrode, Ag wire pseudo-reference electrode, and graphite counter electrode. The working electrode was polished with 0.25 μm diamond polishing paste inside a glove box and then rinsed with acetonitrile. A CHI Instruments 620D potentiostat was used.

Headspace gas analysis was performed using an Agilent Technologies 6850 GC System equipped with a Supelco 10 ft × 1/8 inch carbosieve column with a thermal conductivity detector (TCD). The method for gas analysis was performed with the following parameters: Inlet temperature: 230 °C; Flow: 15.9 mL/min; Oven temperature and ramp program: initial temperature 40 °C, hold 12 minutes; 40 °C/min to 200 °C.; Carrier gas: Ar; Detector: TCD at 250 °C. UltraHigh Purity He gas (99.999%) was used as an internal standard for N_2 quantification. An ultrapure research grade premixed primary gas standard of H_2 (0.499%), He (0.499%), N_2 (4.999%), and Ar (94.003%) was purchased from RedBall Oxygen. The gas response factors for N_2, O_2, and He were determined by injecting 0.10-0.20 mL of the calibration gas and running the GC method described above. The gas retention times of He, O_2, N_2 are 1.1, 6.1 and 6.7 min, respectively. Oxygen and nitrogen could be nearly baseline resolved, thus O_2 and N_2 contaminants from air that were introduced during sample injection were subtracted assuming an air composition of 20.95% O_2 and 78.09% N_2.

General procedure for N_2 forming reactions and headspace analysis:
In an N_2 filled glove box, a J. Young NMR tube was charged with 0.75 mL of a stock solution of **Ph_3C-ArO•** containing 1.100 g of **Ph_3C-ArO•** and 50 mg of hexamethylbenzene (internal standard) dissolved in 5 mL C_6D_6. 10, 25, or 50 μL of a stock solution of (TMP)Ru($^{15}NH_3$)$_2$ (15 mg in 1 mL of C_6D_6) was then added. The tube was then diluted to 0.8 mL with C_6D_6 if needed. The NMR tube was sealed, then degassed by freeze-pump-thaw cycles (3×). The tube was then charged with 1.5 atmospheres of $^{15}NH_3$ or $^{14}NH_3$, carefully tapped and inverted to assist with gas/liquid mixing until the pressure no longer dropped upon exposure to ~1.5 atmospheres. The

tube was sealed then removed from the Schlenk line and placed on a rotator to aid in gas/solvent mixing for 24 hours. The concentration of NH_3 in solution is ~ 0.3 M as judged by internal standard.

The J. Young tube was attached to a gas sampling apparatus that has been described in detail previously.[4] (see Figures S10 and S11 of the Supporting Information). The headspace above the tube was evacuated and sealed off from vacuum, then the J. Young tube was opened. He gas (0.2 mL) was injected into the gas sampling apparatus, mixed into the reaction headspace by withdrawing 0.8 mL into the syringe, and reinjected every 30 seconds for 2 minutes. The headspace was allowed to equilibrate for an additional minute, then the head space was removed using the gas tight syringe, sealed, and injected into the GC for analysis.

Synthesis of (TMP)Ru(CO)($^{15}NH_3$)

Four J. Young tubes were equally charged (~1.25 mL each) with a stock solution of (TMP)Ru(CO) (0.053 mmol, 50 mg) dissolved in C_6D_6 (5 mL). The tubes were degassed by three consecutive freeze-pump-thaw cycles, then attached to a low-volume gas addition manifold and were pressurized to approximately 1 atm with $^{15}NH_3$ or NH_3. The tubes were then placed on a rotator to aid in gas-liquid mixing for approximately 30 minutes. The solutions were transferred to a scintillation vial and dried under reduced pressure to yield 50 mg of (TMP)Ru(CO)(NH_3) as a red-purple solid in 99% yield. (TMP)Ru(CO)(NH_3) loses NH_3 over prolonged exposure under vacuum.

^{1}H NMR (C_6D_6, 25° C): δ 8.71 (s, 8H), 7.19 (s, 4H), 7.07 (s, 4H), 2.44 (s, 12H), 2.04 (s, 12H), 1.87 (s, 12H), -5.54 (d, J = 66.6 Hz, 3H).

$^{13}C\{^1H\}$ NMR (C_6D_6, 25° C): δ 144.19, 140.26, 139.26, 138.22, 137.47, 131.44, 128.52, 119.45, 21.96, 21.65, 21.52.

^{15}N NMR (C_6D_6, 25° C): δ -392.3 (q, J = 67.9 Hz).

Synthesis of (TMP)Ru(NH_3)$_2$

Four J. Young tubes were equally charged (~1.25 mL) with a stock solution of (TMP)Ru(CO) (0.053 mmol, 50 mg) dissolved in C_6D_6 (5 mL). The tubes were degassed by three freeze-pump-thaw cycles, then attached to a low-volume gas addition manifold and were pressurized to approximately 1 atm with $^{15}NH_3$ or NH_3. The tubes were then placed next to a medium pressure Hg lamp contained in a water-cooled quartz jacket and photolyzed for approximately 6 hours, or placed inside a Rayonet photochemical reactor equipped with 250 nm lightbulbs and photolyzed for 2 days. The lamp, or Rayonet, was turned off, and the tubes removed. The tubes were then cooled to -35 ºC, quickly degassed, and then photolyzed again until complete conversion. This process is repeated until full conversion is achieved. Reaction progress can be monitored by NMR spectroscopy. Upon completion, the tubes were evacuated to dryness yielding 48 mg (96%) of crude (TMP)Ru(NH_3)$_2$ as a red/purple solid. Single crystals were grown by slow evaporation of a concentrated THF solution of (TMP)Ru(NH_3)$_2$. (TMP)Ru(NH_3)$_2$ loses NH_3 after prolonged exposure under vacuum.

^{1}H NMR (C_6D_6, 25° C): δ 8.31 (s, 8H), 7.2 (s, 8H), 2.46 (s, 12H), 2.12 (s, 24H), -6.88 (d, J_{NH} = 68.2 Hz, 6H).

$^{13}C\{^1H\}$ NMR (C_6D_6, 25° C): δ 144.50, 139.46, 138.96, 136.83, 131.53, 128.22, 119.92, 21.84, 21.56.

$^{15}N\{^1H\}$ NMR (C_6D_6, 25° C): δ -427.8

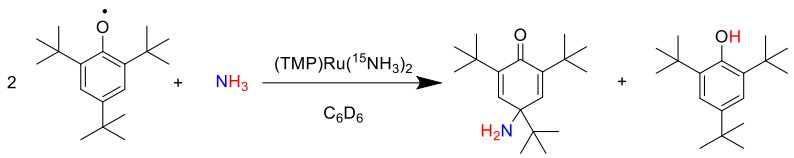

Synthesis of 4-amino-2,4,6-tri-tert-butylcyclohexa-2,5-dien-1-one (RNH_2)

In an N_2 filled glove box, a J. Young NMR tube was charged with 1.0 mL of a stock solution of **ArO•** containing 600 mg of **ArO•** and 30 mg of hexamethylbenzene (internal standard) dissolved in 5 mL C_6D_6. 15 µL of a stock solution of (TMP)Ru($^{15}NH_3$)$_2$ (15 mg in 1 mL of C_6D_6) was then added. The tube was degassed by three freeze-pump-thaw cycles. Then the tube was charged with 1.5 atmospheres of $^{15}NH_3$ or NH_3, carefully tapped and inverted to assist with gas/liquid mixing until the pressure no longer dropped upon exposure to ~1.5 atmospheres, then the headspace was pressurized to 1.5 atmospheres, and the tube was sealed. The tube was removed from the Schlenk line and placed on a rotator to aid in gas-liquid mixing for 3 days. Reaction progress can be monitored by ^1H NMR spectroscopy, or by visually watching the blue color of the radical disappear. Upon reaction completion, the mixture was transferred to a separatory funnel, and 10 mL of Et_2O was added, followed by 10 mL of 2 M HCl. The funnel was shaken and then the ether layer was separated and washed 3× with DI water. All the aqueous fractions were combined and neutralized with K_2CO_3. The resulting solution was then extracted three times with 10 mL Et_2O. The ether layers were combined and dried over $MgSO_4$. Finally, the solution was filtered over Celite and evacuated to dryness to yield **RNH_2** (internal standard: 65 %) as a white solid.

^1H NMR (C_6D_6, 25° C): δ 6.43 (s, 2H), 1.35 (s, 18H), 0.86 (s, 9H), 0.72 (d, J = 64.4 Hz, 2H).

$^{13}C\{^1H\}$ NMR (C_6D_6, 25° C): 186.06, 146.48, 144.08, 57.06 (d, J_{CN} = 15 Hz), 39.24, 35.13, 29.86, 25.66.

^{15}N NMR (C_6D_6, 25° C): -341.33 (t, J_{NH} = 64.4 Hz).

Synthesis of 2,6-di-*tert*-butyl-4-tritylphenoxyl radical (Ph_3C-ArO•)

The synthesis of 2,6-di-*tert*-butyl 4-trityl phenoxyl[5] radical involved a modified procedure of 2,4,6-*tri*-t-butylphenoxyl radical.[2] The parent phenol, 2,6-di-*tert*-butyl 4-trityl phenol (**Ph_3C-ArOH)**, 2.147 g, 4.79 mmol), was dissolved in 80 mL benzene, and 15 mL of 1M NaOH was added. The solution was degassed using two freeze-pump-thaw cycles. The solution was frozen again, and potassium ferricyanide (3.94 g, 11.97 mmol) was added as a solid against a counter current of N_2. The headspace was evacuated and then backfilled with nitrogen two times. Upon warming to room temperature, the reaction was stirred for two hours under nitrogen. The solvent was removed under vacuum, and the flask transferred to a glovebox where 100 mL of diethyl ether was added, and the solution was then filtered Note that it is important to ensure all water is removed before filtration. The diethyl ether was removed under vacuum from the filtrate, and the dark green solid was dissolved in approximately 100 mL acetonitrile. Dark green crystals of **Ph_3C-ArO•** grew overnight in the dark at -35 °C. The crystals were isolated on a medium porosity frit, dried, and then dissolved in pentane and filtered once more. The pentane solution was dried under vacuum to yield **Ph_3C-ArO•** as a dark green solid (1166 mg, 54%). Single crystals of **Ph_3C-ArO•** were grown from MeCN at -35 °C.

Elemental Analysis: C, 88.54; H, 7.88; O, 3.57. Found: C, 87.59; H, 7.90.

UV-Vis: λ_{max} = 423 nm (ε = 2475 $M^{-1}cm^{-1}$). λ = 632 nm (ε = 420 $M^{-1}cm^{-1}$).

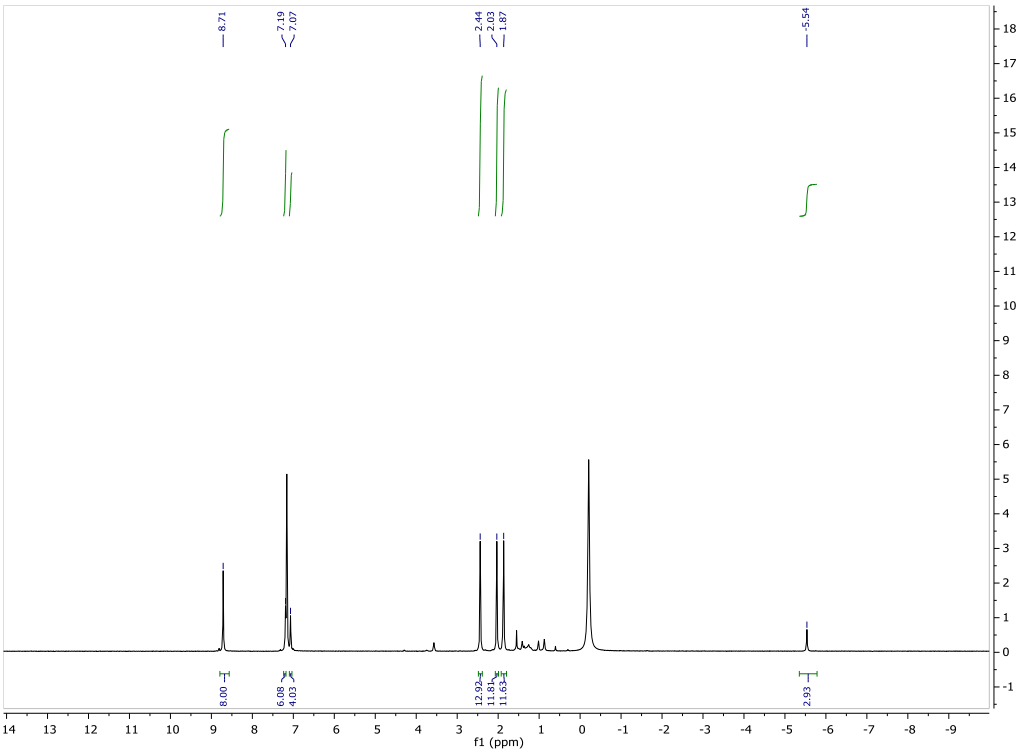

Figure S1: In situ ^{1}H NMR spectrum of (TMP)Ru(CO)(NH_3) in C_6D_6 with excess NH_3.

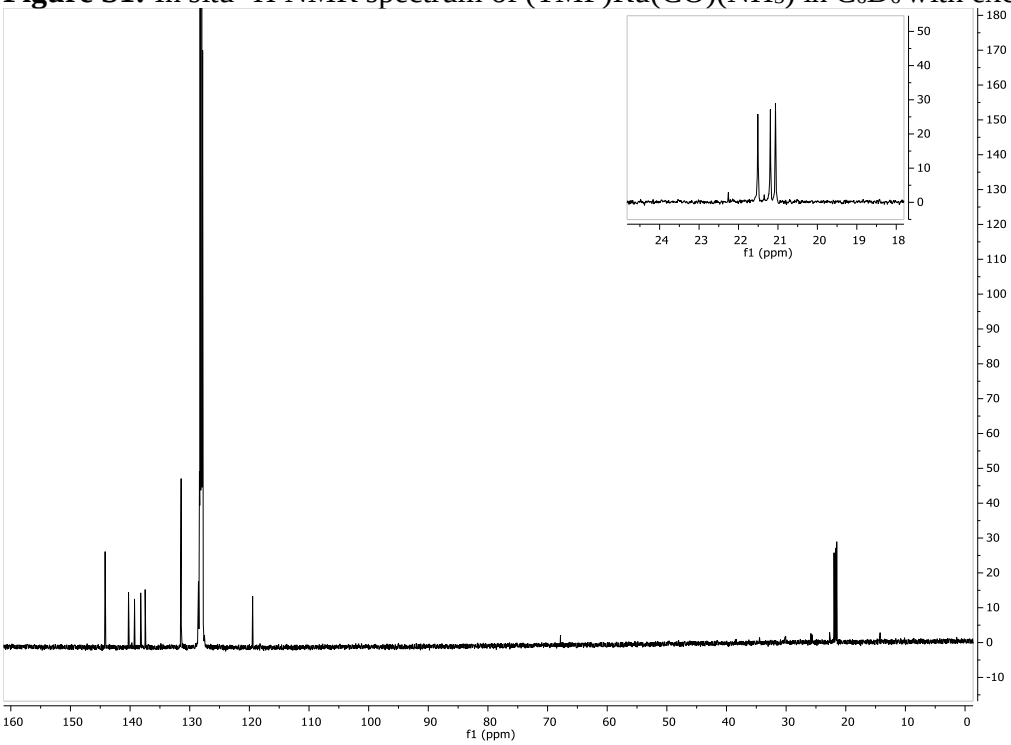

Figure S2: $^{13}C\{^{1}H\}$ NMR spectrum of (TMP)Ru(CO)(NH_3) in C_6D_6. Alkyl region expanded for clarity.

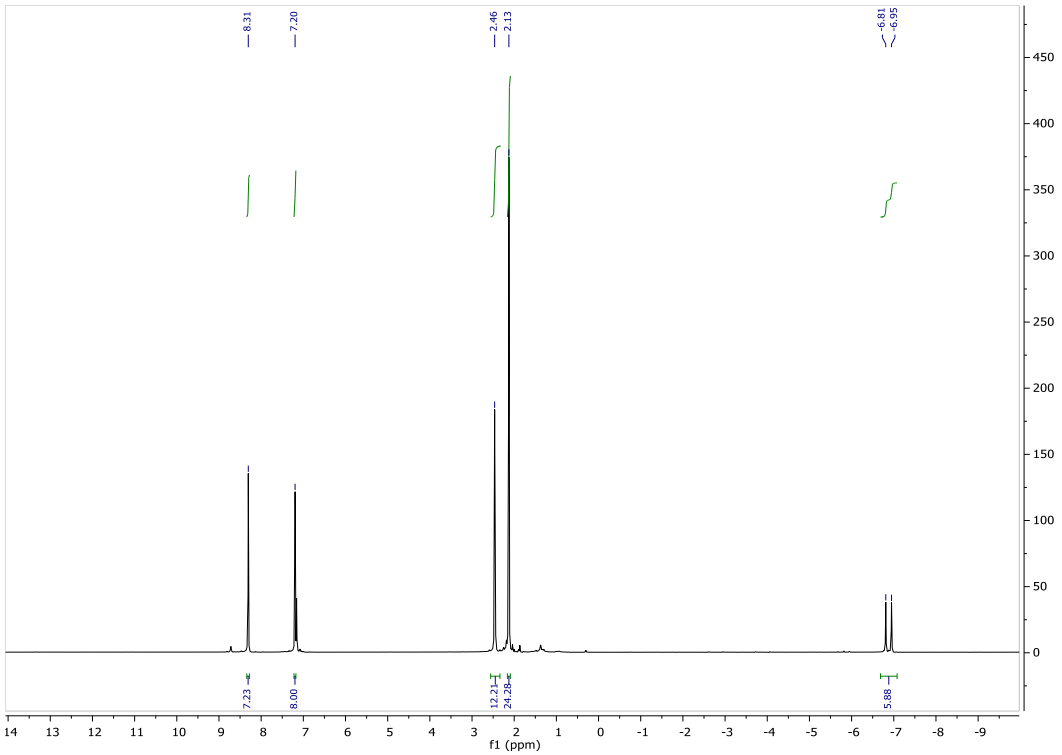

Figure S3: ^{1}H NMR spectrum of (TMP)Ru($^{15}NH_3$)$_2$ in C_6D_6.

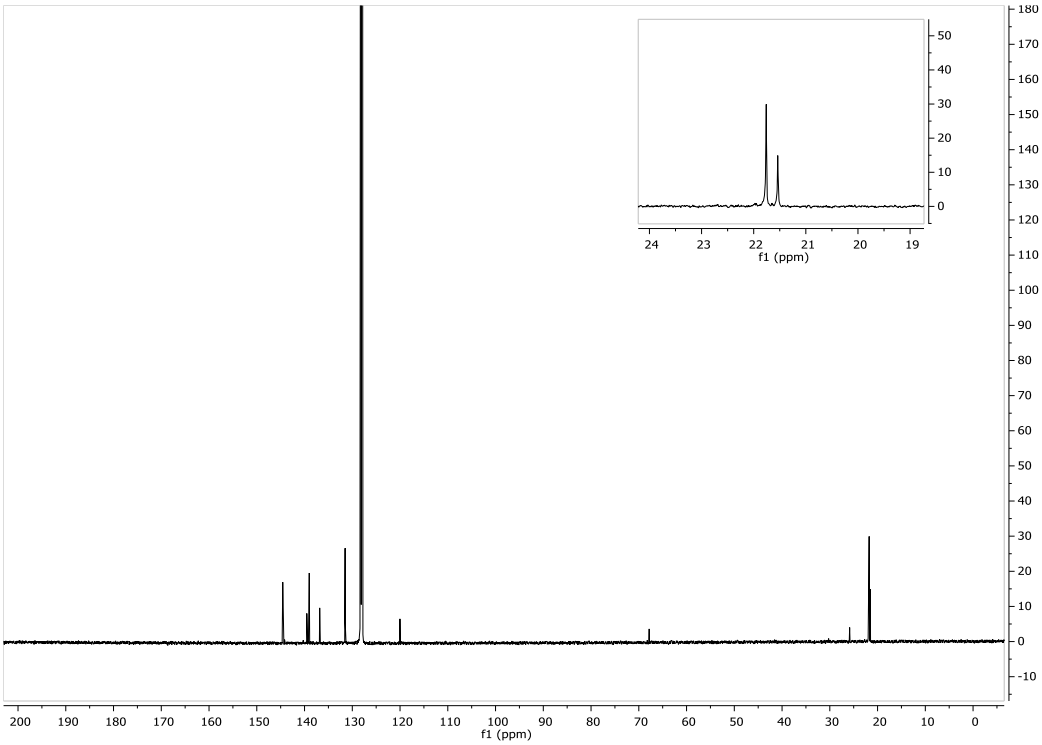

Figure S4: $^{13}C\{^{1}H\}$ NMR spectrum of (TMP)Ru($^{15}NH_3$)$_2$ in C_6D_6. Alkyl region expanded for clarity.

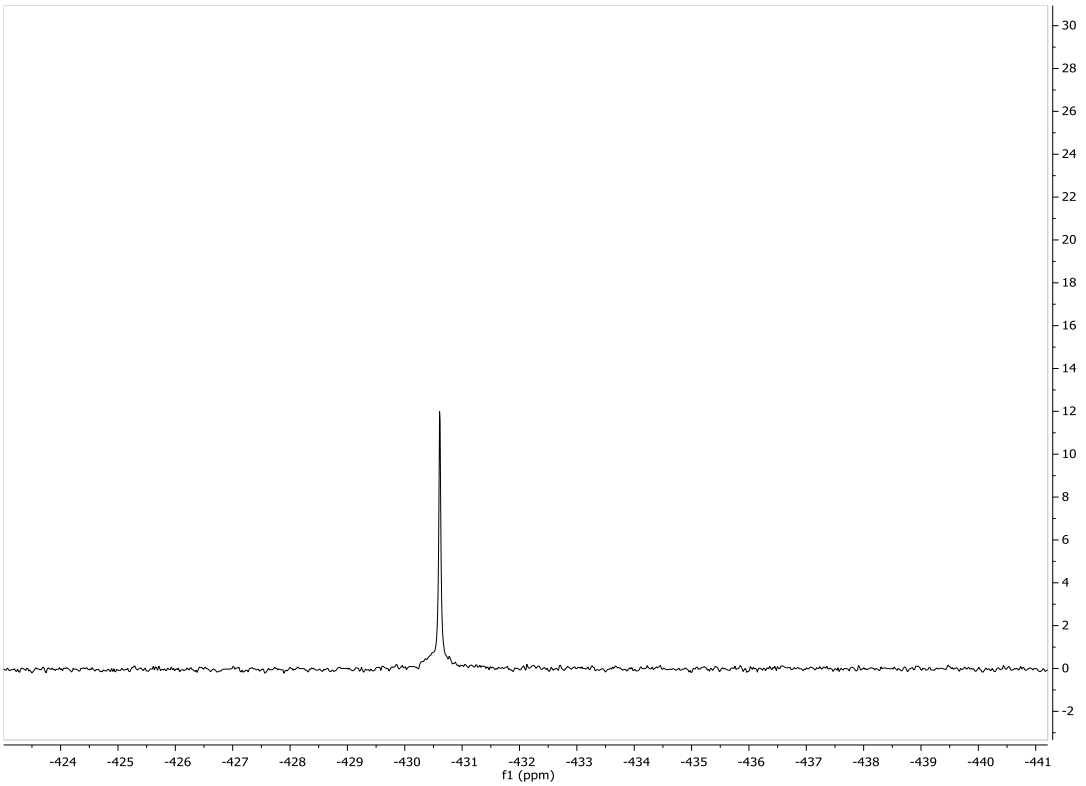

Figure S5: $^{15}N\{^{1}H\}$ NMR spectrum of (TMP)Ru($^{15}NH_3$)$_2$ in C_6D_6.

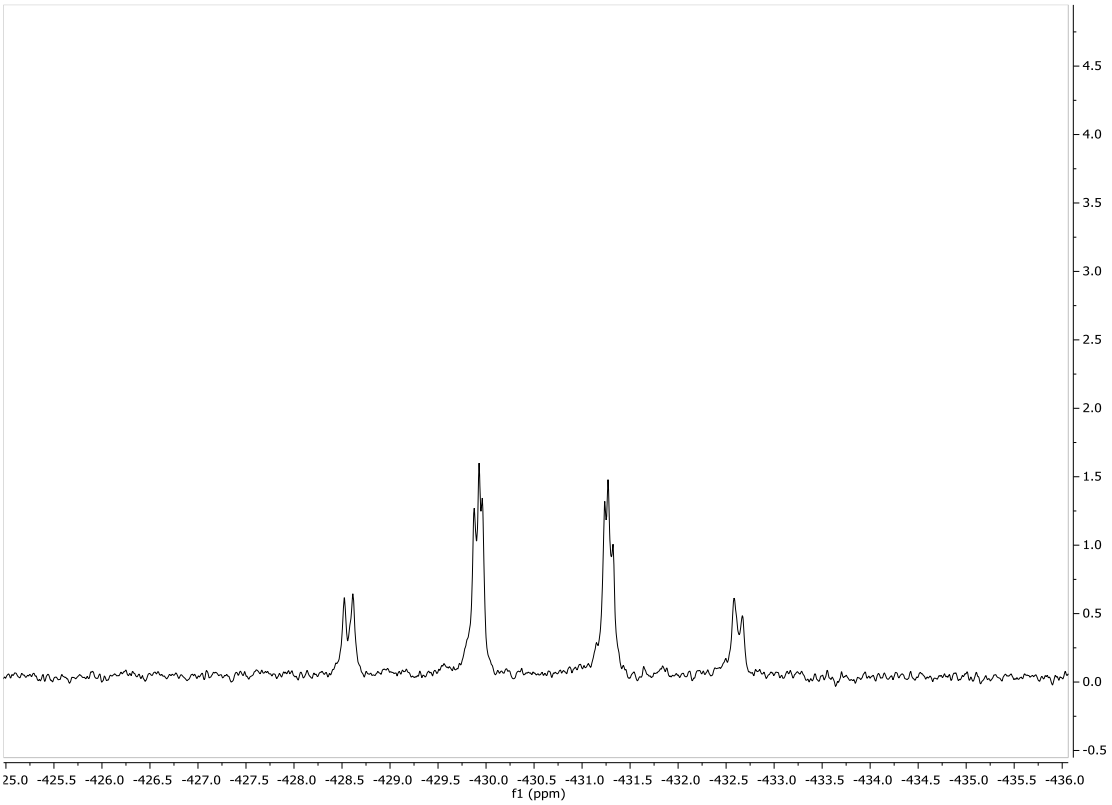

Figure S6: ^{15}N NMR spectrum of (TMP)Ru($^{15}NH_3$)$_2$ in C_6D_6 displaying second-order coupling.

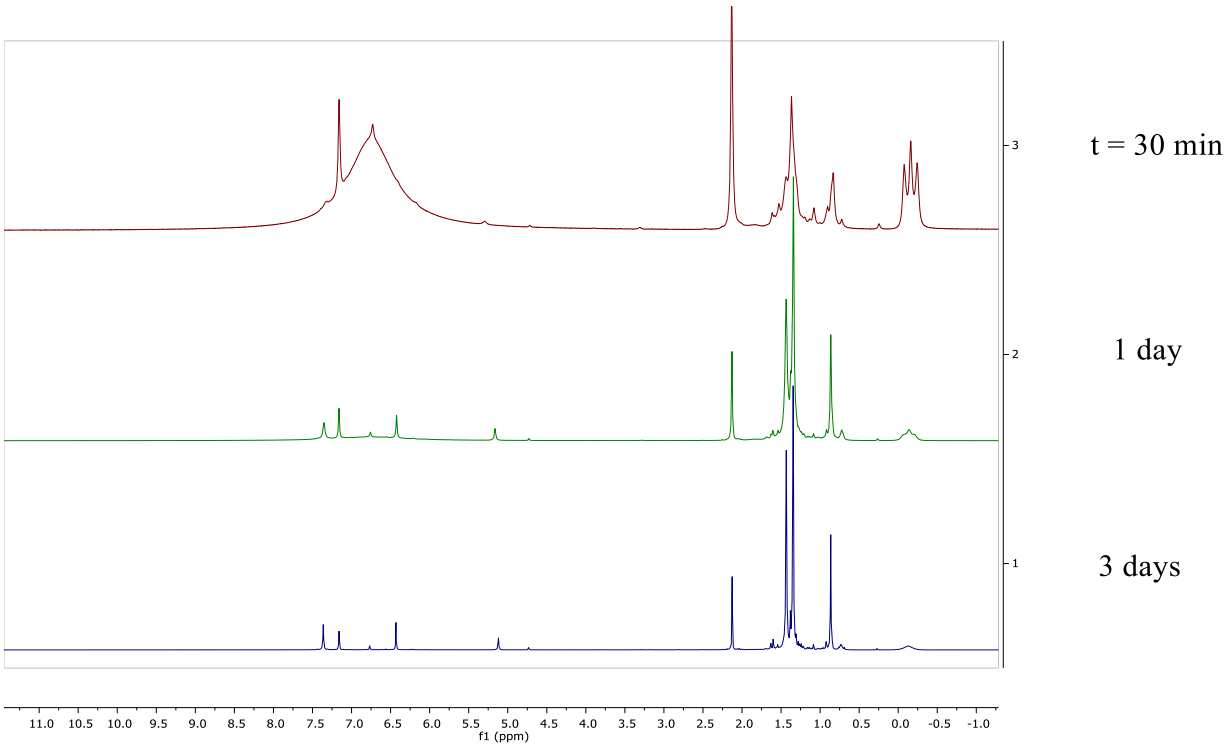

Figure S7: ^{1}H NMR spectrum of catalytic C-N coupling over time.

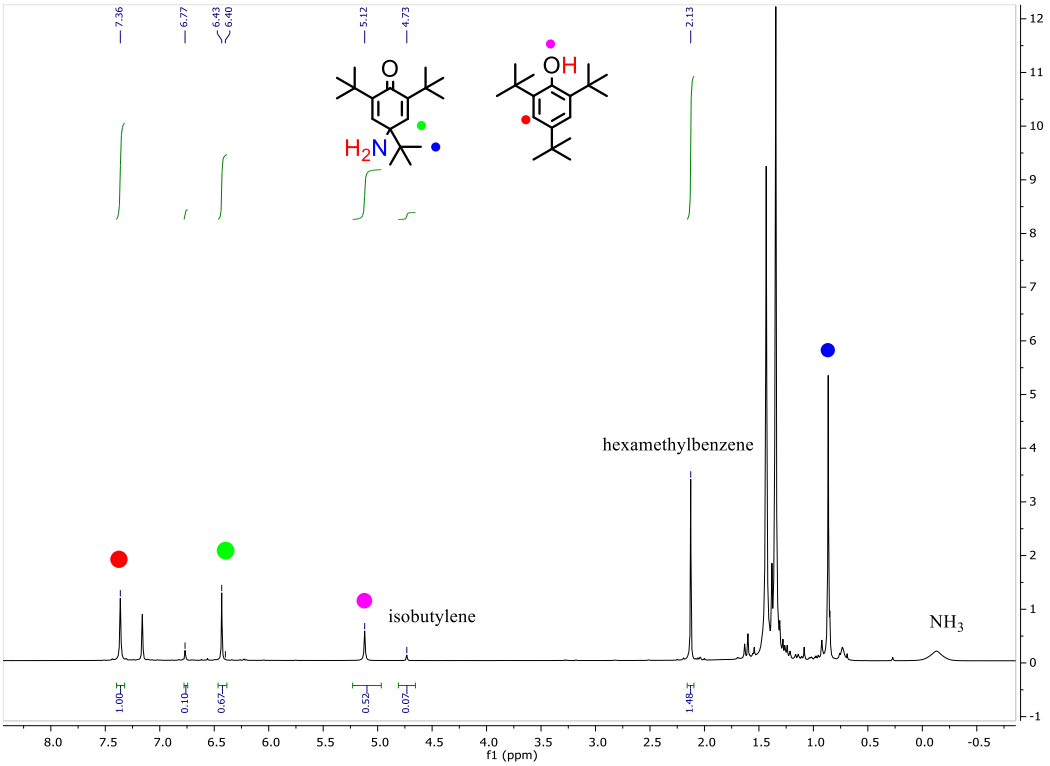

Figure S8: ^{1}H NMR spectrum of catalytic C-N coupling after 3 days.

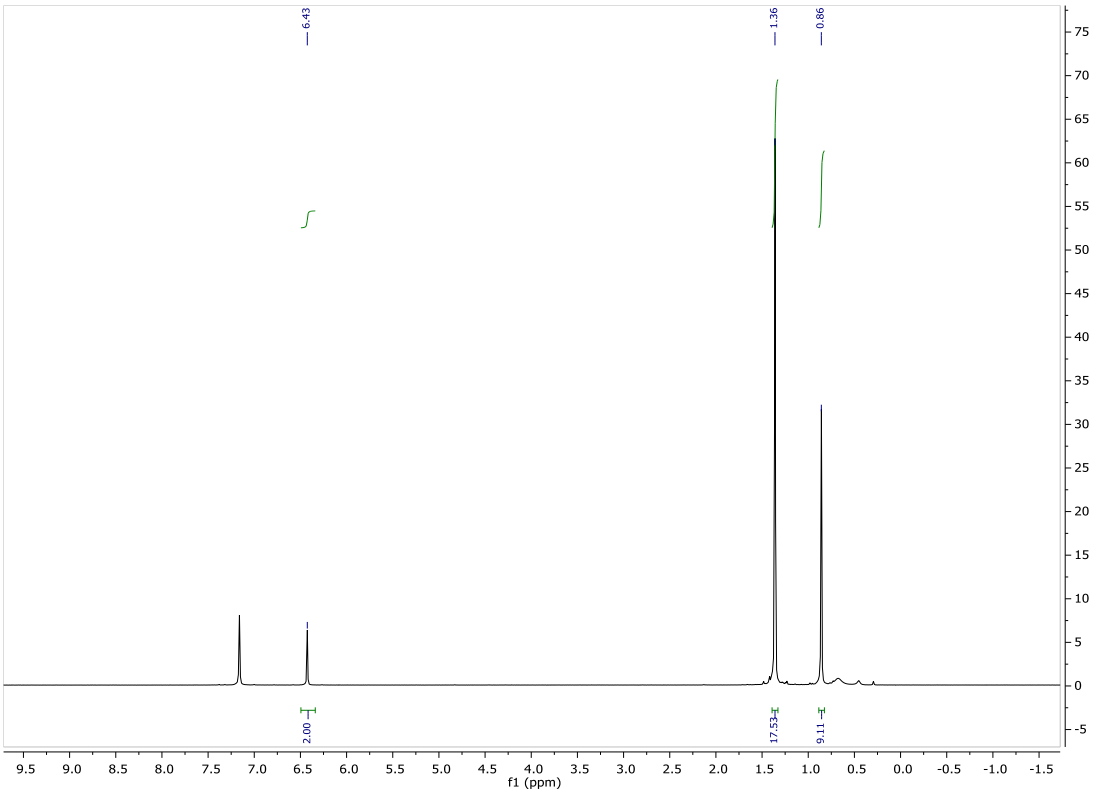

Figure S9: ^{1}H NMR spectrum of $\mathbf{R^{15}NH_2}$ in C_6D_6.

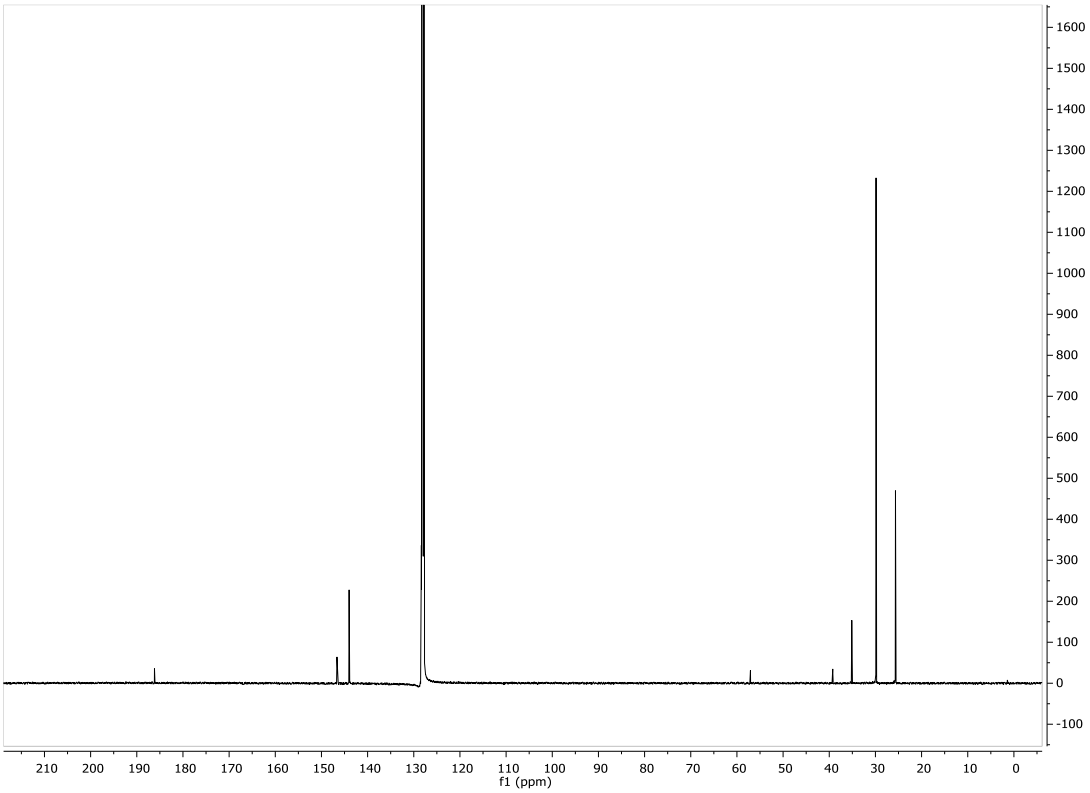

Figure S10: $^{13}C\{^{1}H\}$ NMR spectrum of $\mathbf{R^{15}NH_2}$ in C_6D_6.

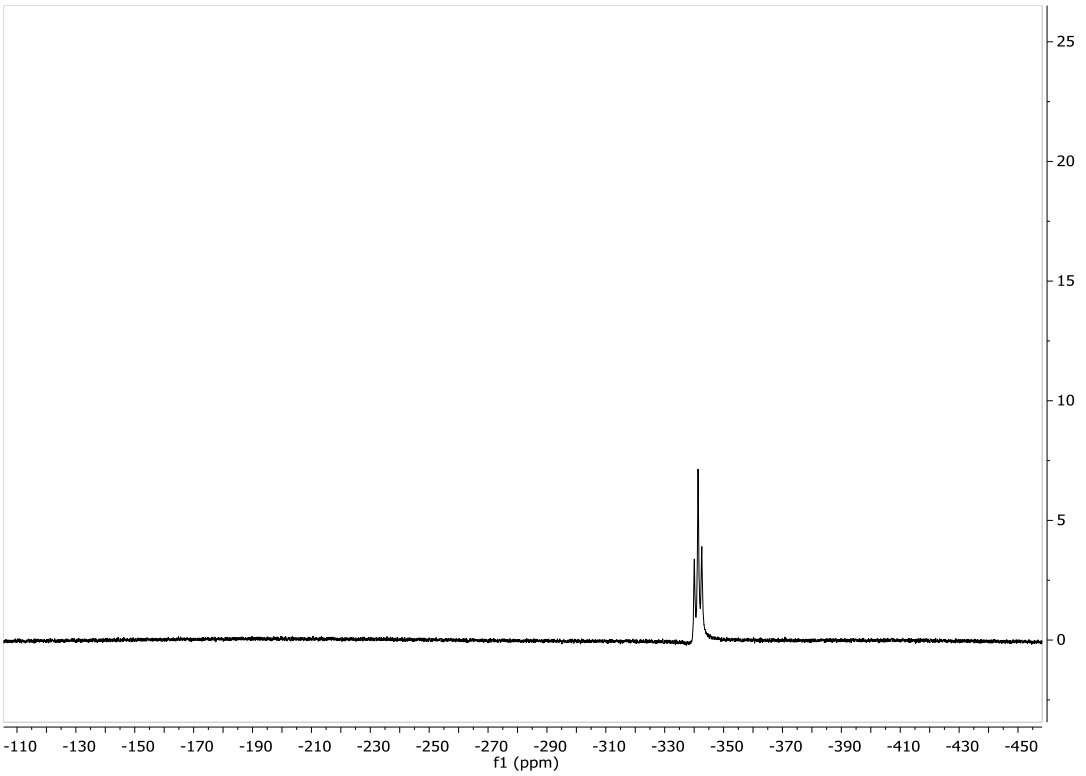

Figure S11: ^{15}N NMR spectrum of **R^{15}NH$_2$** in C_6D_6.

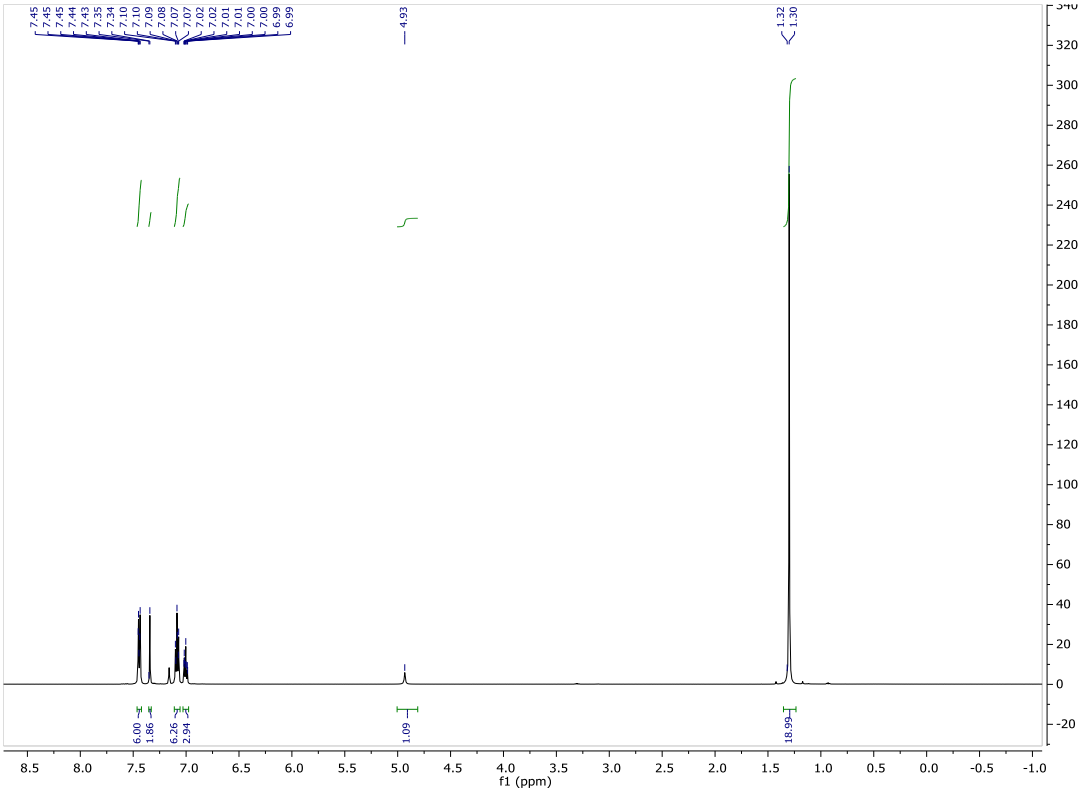

Figure S12: ^{1}H NMR spectrum of **Ph$_3$C-ArOH** in C_6D_6.

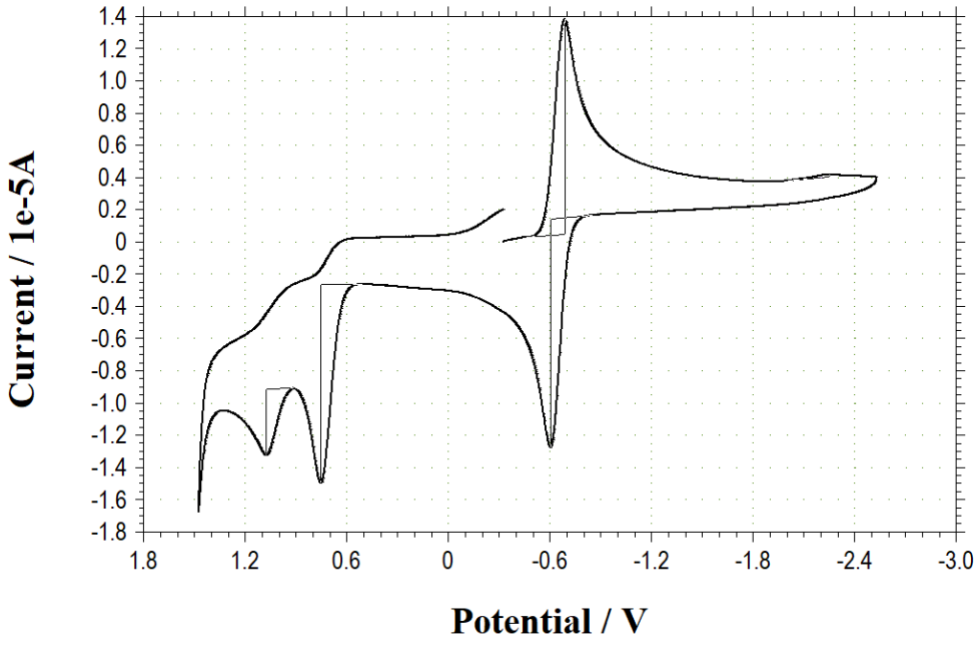

Figure S13: Cyclic voltammogram of **Ph_3C-ArO•** (3.3 mM) in MeCN with 100 mM $(NBu_4)PF_6$. Scan rate = 500 mV/s. $E_{1/2}$ = -0.645 V. Referenced vs. $Cp_2Fe^{+/0}$ = 0.0 V.

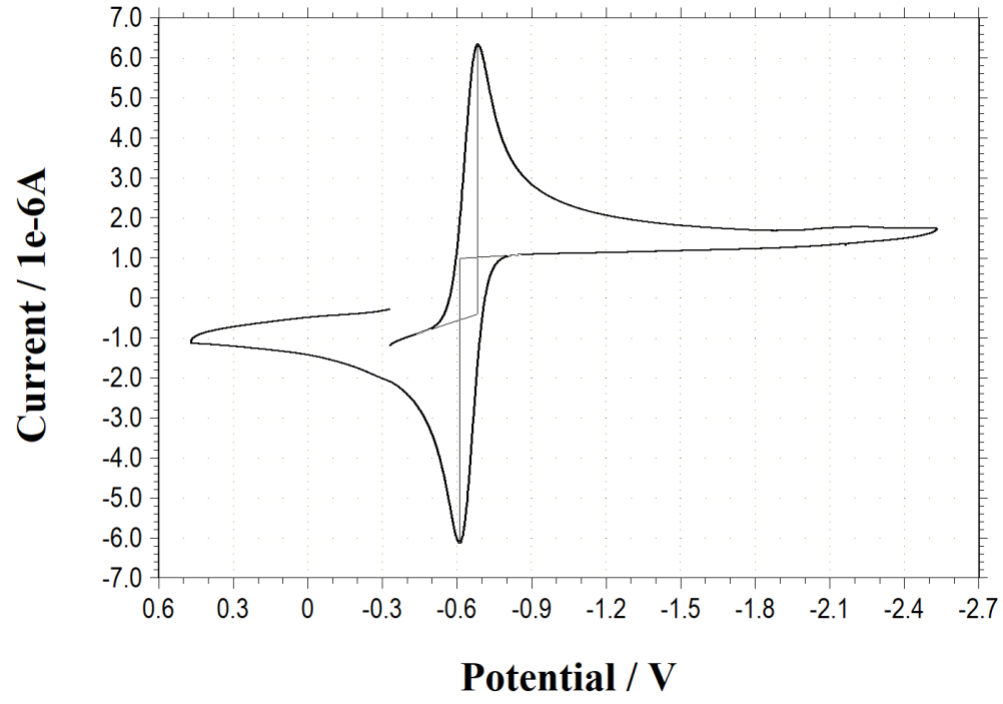

Figure S14: Cyclic voltammogram of the **Ph_3C-ArO•/Ph_3C-ArO-** (phenoxyl/phenoxide) couple at 100 mV/s in MeCN with 100 mM $(NBu_4)PF_6$. $E_{1/2}$ = -0.645 V. Referenced vs. $Cp_2Fe^{+/0}$ = 0.0 V.

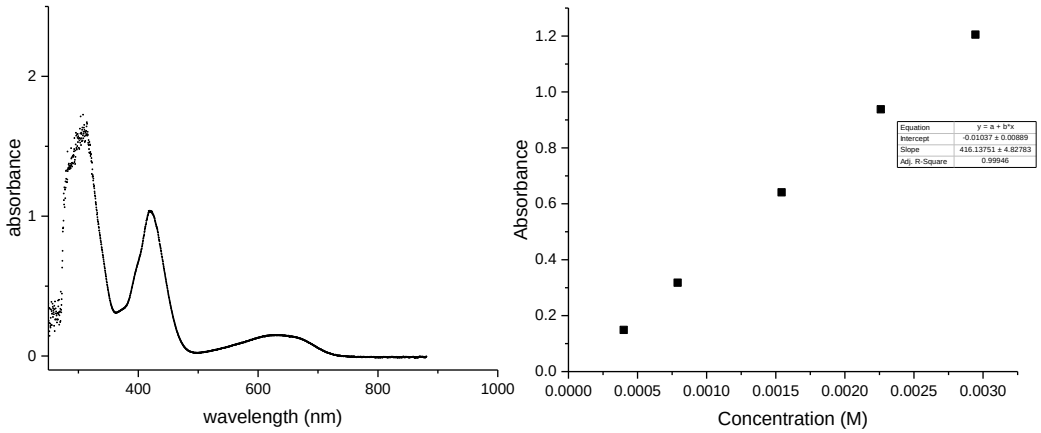

Figure S15: UV-Vis (left) and Beer's Law plot (right) of **Ph_3C-ArO•** in C_6D_6. λ_{max} = 423 nm (ε = 2475 $M^{-1}cm^{-1}$). λ = 632 nm (ε = 420 $M^{-1}cm^{-1}$).

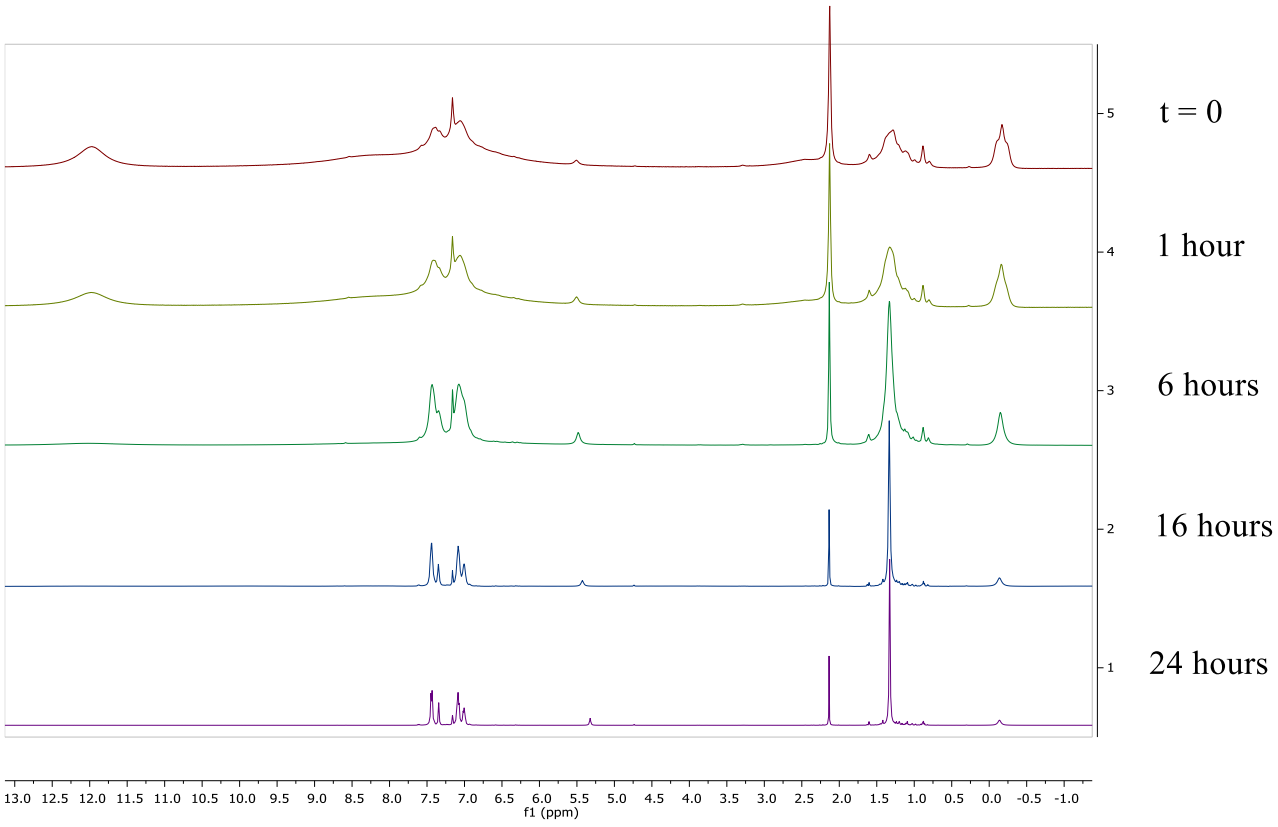

Figure S16: ^{1}H NMR spectrum of 1.0 mM [Ru] catalytic ammonia oxidation run over time.

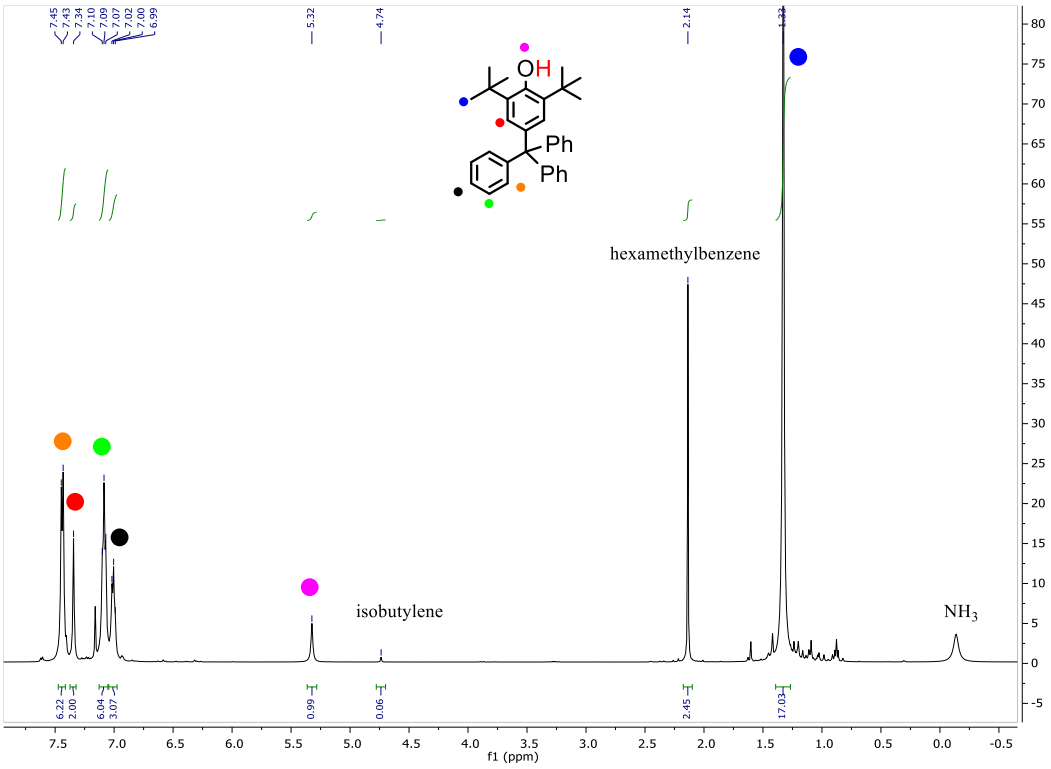

Figure S17: ^{1}H NMR spectrum of 1.0 mM [Ru] catalytic ammonia oxidation reaction after 24 hours.

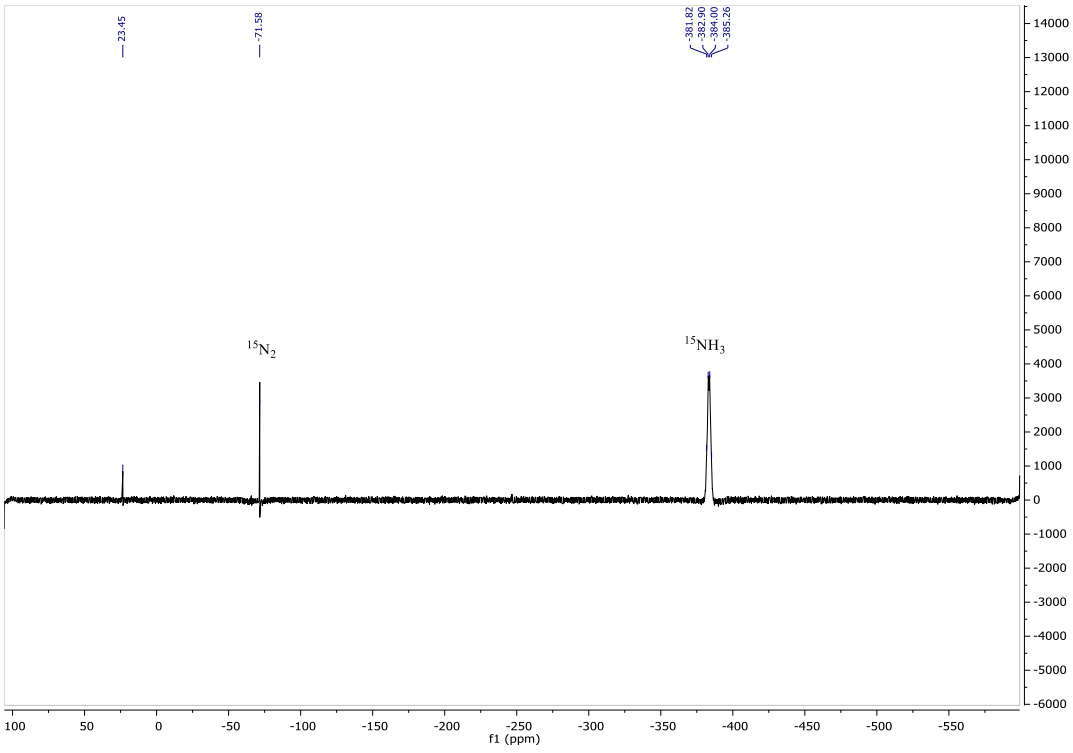

Figure S18: Overnight ^{15}N NMR spectrum of 1.0 mM [Ru] catalytic ammonia oxidation experiment using $^{15}NH_3$.

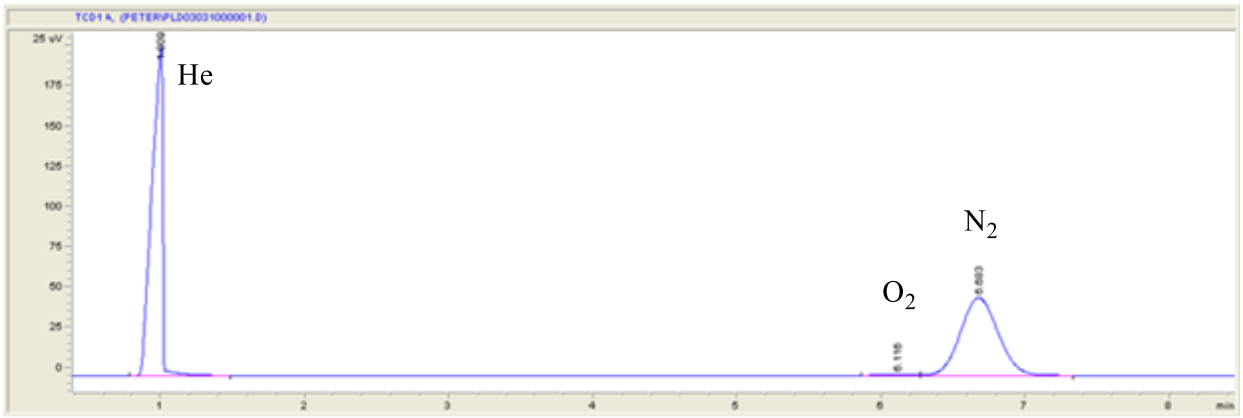

Figure S19: Example GC trace from a 1.0 mM [Ru] catalytic ammonia oxidation experiment showing He, O_2, and N_2.

Table S1. GC Results of N_2 formed in catalytic ammonia oxidation.

[Ru]	Trial #	moles N_2 Formed	Turnovers	Average	Standard Deviation
1.0 mM	A	3.27×10^{-5}	39.9	40	0.5
	B	3.21×10^{-5}	39.2		
	C	3.29×10^{-5}	40.2		
0.5 mM	A	3.28×10^{-5}	80.2	75	7
	B	2.86×10^{-5}	69.9		
0.25 mM	A	2.57×10^{-5}	125	125	5
	B	2.64×10^{-5}	130		
	C	2.44×10^{-5}	120		

Table S2. ^{1}H NMR spectroscopy results from catalytic ammonia oxidation experiments with 1.0 mM [(TMP)Ru(NH_3)$_2$] measured at t = 1 day.

	A	B	C
% yield 4-trityl-ArOH[a,b]	88	91	92
% yield isobutylene[a,b]	2.2	2.2	2.2
Turnovers of N_2[c]	39.9	39.2	40.2

[a] Based on NMR spectra with internal standard, recorded when all radical is quenched.
[b] Yields are calculated based on phenoxyl radical added.
[c] Determined by GC with He internal standard. Catalytic turnovers are determined by dividing total mmol N_2 observed by the total mmol of Ru (mmol N_2/mmol Ru).

X-Ray Crystallography: General Considerations.

A black plate of (TMP)Ru($^{15}NH_3$)$_2$, a green block of **Ph_3C-ArO•** and a colorless block of **Ph_3C-ArOH** were mounted on a loop with oil. Data was collected at 133 K on a Nonius Kappa CCD FR590 single crystal X-ray diffractometer, Mo-radiation, or a Bruker X-ray diffractometer at 100 K, Mo radiation. The data intensity was corrected for absorption and decay (SADABS).[6] Final cell constants were obtained from least-squares fits from all reflections. Crystal structure solution was done through intrinsic phasing (SHELXT-2014/5),[7] which provided most nonhydrogen atoms. Full matrix least-squares/difference Fourier cycles were performed (using SHELXL-2016/6 and GUI ShelXle)[8-9] to locate the remaining non-hydrogen atoms. All non-hydrogen atoms were refined with anisotropic displacement parameters. Hydrogen atoms were placed in ideal positions and refined as riding atoms with relative isotropic displacement parameters. Details regarding refined data and cell parameters are available in Table S3.

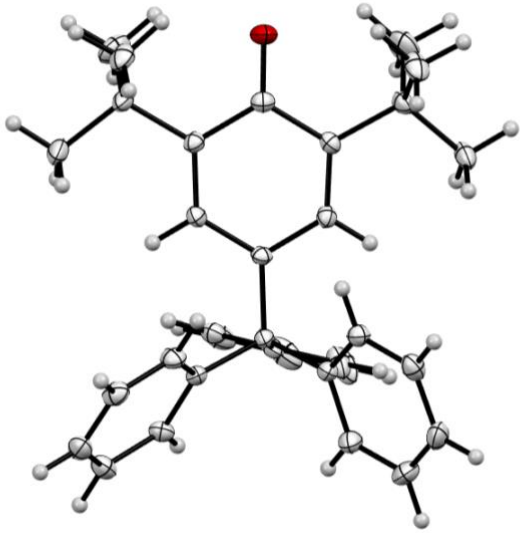

Figure S20. 50% ellipsoid drawing of **Ph_3C-ArO•**. MeCN and second molecule in the asymmetric unit not shown.

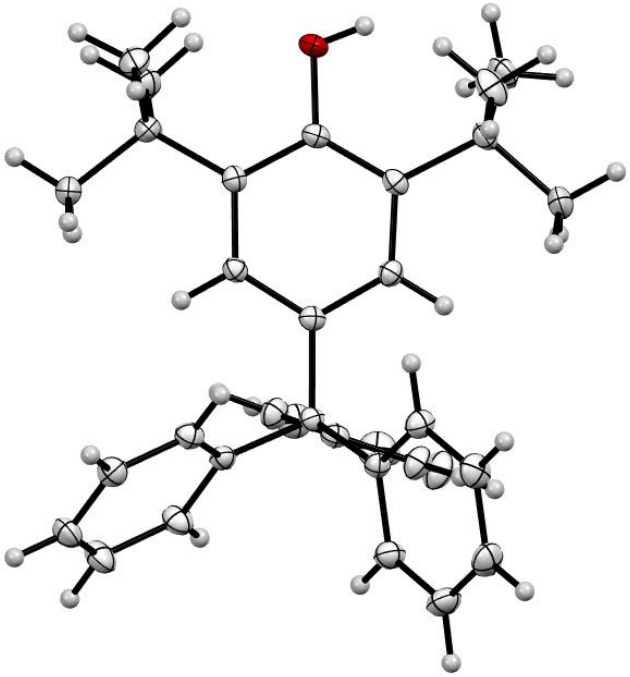

Figure S21. 50% ellipsoid drawing of **Ph_3C-ArOH**.

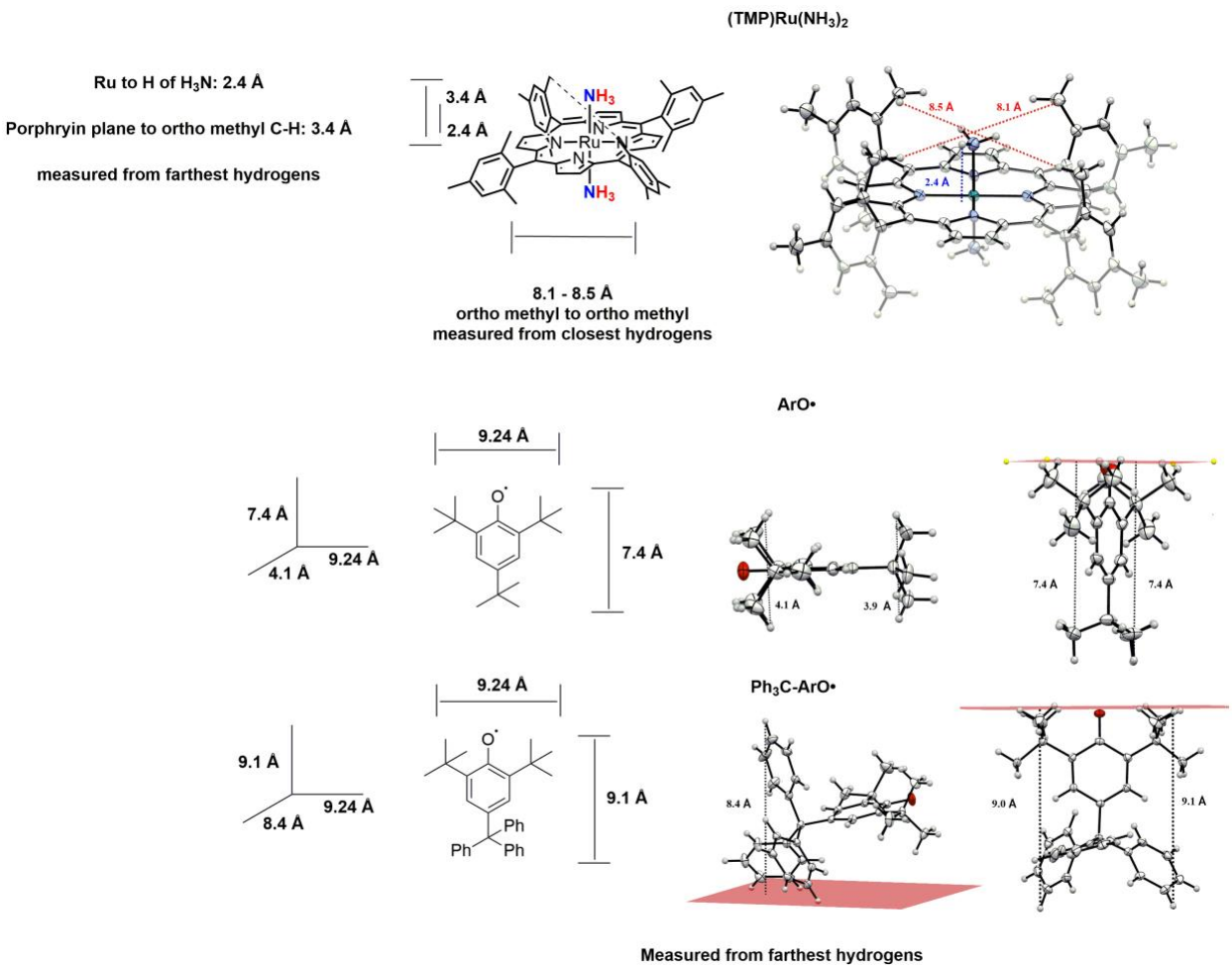

Figure S22. Size comparison of **(TMP)Ru(NH3)2, Ph3C-ArO•,** and **Ph3C-ArOH.**

Table S3. Crystal and refinement data for complexes **TMPRu(NH$_3$)$_2$, Ph$_3$C-ArO•,** and **Ph$_3$C-ArOH.**

	(TMP)Ru(NH$_3$)$_2$	**Ph$_3$C-ArO•**	**Ph$_3$C-ArOH**
CCDC Number	1972399	1972396	1972397
Empirical Formula	$C_{56}H_{58}N_6Ru$ • 4(C_4H_8O)	2($C_{33}H_{35}O$) • (C_2H_3N)	$C_{33}H_{36}O$
Formula weight	1204.56	936.27	448.62
T (K)	130(2)	100(2)	100(2)
a, Å	11.2702(7)	9.8007(8)	9.6158(9)
b, Å	11.8317(7)	15.2538(10)	10.5411(10)
c, Å	12.8794(10)	18.0720(12)	13.8499(14)
α, deg	100.208(3)	90	99.752(3)
β, deg	90.767(3)	90.781(3)	106.021(4)
γ, deg	110.714(3)	90	90 98.980(4)
Volume, Å^3	1575.56(19)	2701.5(3)	1299.0(2)
Z	1	2	2
Crystal System	Triclinic	Monoclinic	Triclinic
Space Group	P-1	P2(1)	P-1
d_{calc}, g/cm^3	1.270	1.151	1.147
θ Range, deg	2.223 to 28.379	2.349 to 28.211	2.815 to 28.2715
μ, mm^{-1}	0.303	0.068	0.067
Abs. Correction	Multi-scan	Multi-scan	Multi-scan
GOF	1.027	1.016	1.031
R_1 ,[a]	$R1$ = 0.0643	$R1$ = 0.0501	$R1$ = 0.0521
wR_2 [b] [I>2σ (I)]	$wR2$ = 0.1407	$wR2$ = 0.1263	$wR2$ = 0.1433

[a] $R_1 = \sum||F_o| - |F_c||/\sum|F_o|$. [b] $wR_2 = [\sum[w(F_o^2-F_c^2)^2]/\sum[w(F_o^2)^2]]^{1/2}$.

Computational Methods

Density functional theory calculations were used to probe the bond dissociation free energy (BDFE) values and N–C bond formation. The B3LYP functional[10] was used for all calculations employed with Grimme's D3 dispersion correction with Becke-Johnson damping.[11-12] Geometries were optimized using the 6-31G**[13] basis set on all non-metal atoms. The Karlsruhe def2 double-ζ basis set[14] with polarization and associated ECP[15] was used for Ru. Analytical frequencies were calculated at the same level of theory to give entropic and enthalpic contributions at 298.15K, as well as to ensure intermediates were minima on the potential energy surface. The SMD implicit solvation model[16] was used to calculate single point solvation energies in benzene. Finally, single point large basis set electronic energies were calculated using the Karlsruhe triple-ζ def2-TZVP[14] on all atoms and the associated ECP on Ru.[15] These energies, combined with the enthalpic and entropic terms, give free energies of the relevant molecules. Mid- and high-spin geometries were calculated to ensure that the correct spin state was chosen, but for all complexes the low-spin variation was the lowest in energy and are reported here. All calculations were completed in Orca 4.0.2[17] Bond dissociation free energies were referenced to 2,4,6-tri-*tert*-butyl phenoxyl radical using the experimental BDFE in benzene.[18]

Molecule Geometries

All molecule cartesian coordinates are given in an associated XYZ file. This file can be opened with any free molecular GUI, including Mercury (https://www.ccdc.cam.ac.uk/mercury/), Avogadro, or MacMolPLT.

Table S4. Computed Free Energies

Molecule	Free Energy [kcal mol^{-1}]
(TMP)Ru(NH_3)$_2$	-1626044.0
(TMP)Ru(NH_2)(NH_3)	-1625652.6
(TMP)Ru(NH)(NH_3)	-1625250.1
(TMP)Ru(NH_2)(NH_2)	-1625256.7
(TMP)Ru(N)(NH_3)	-1624865.7
(TMP)Ru(NH_2ArO)(NH_3)	-2113903.2
(TMP)Ru(NHArO)(NH_3)	-2113518.4
(TMP)Ru(NH_2ArO)(NH_2)	-2113513.2

References:

1. Camenzind, M. J.; James, B. R.; Dolphin, D., Synthesis and reactivity of a monomeric 14-electron 'bare' ruthenium(II) porphyrin complex; reversible binding of dinitrogen to form mono- and bis-dinitrogen complexes. *J.Chem. Soc., Chem. Commun.* **1986,** 1137-1139.

2. Manner, V. W.; Markle, T. F.; Freudenthal, J. H.; Roth, J. P.; Mayer, J. M., The first crystal structure of a monomeric phenoxyl radical: 2,4,6-tri-tert-butylphenoxyl radical. *Chem. Commun.* **2008,** 256-258.

3. Cook, C.; Gilmour, N., Notes- Oxidation of Hindered Phenols. X. Effect of 4-Substituents Upon the Behavior of 2,6-Di-t-butylphenoxy Radicals. *J. Org. Chem.* **1960,** *25*, 1429-1431.

4. Johnson, S. I.; Heins, S. P.; Klug, C. M.; Wiedner, E. S.; Bullock, R. M.; Raugei, S., Design and reactivity of pentapyridyl metal complexes for ammonia oxidation. *Chem. Commun.* **2019,** *55*, 5083-5086.

5. Teuber, H.-J.; Gross, H.-J., Beweis des monovalenten Charakters von Oxidationsreaktionen mit Kalium-nitrosodisulfonat durch ESR-Messungen, insbesondere an diffundierenden Lösungen. *Chem. Ber.* **1975,** *108*, 2097-2106.

6. Blessing, R., An empirical correction for absorption anisotropy. *Acta Crystallogr., Sect. A: Found. Crystallogr.* **1995,** *51*, 33-38.

7. Sheldrick, G., SHELXT - Integrated space-group and crystal-structure determination. *Acta Crystallogr., Sect. A: Found. Crystallogr.* **2015,** *71*, 3-8.

8. Sheldrick, G. M., Crystal structure refinement with SHELXL. *Acta crystallographica. Section C, Structural chemistry* **2015,** *71*, 3-8.

9. Hübschle, C. B.; Sheldrick, G. M.; Dittrich, B., ShelXle: a Qt graphical user interface for SHELXL. *J. Appl. Crystallogr.* **2011,** *44*, 1281-1284.

10. Becke, A. D., Density-functional thermochemistry. III. The role of exact exchange. *J. Chem. Phys.* **1993,** *98*, 5648-5652.

11. Grimme, S.; Antony, J.; Ehrlich, S.; Krieg, H., A consistent and accurate ab initio parametrization of density functional dispersion correction (DFT-D) for the 94 elements H-Pu. *J. Chem. Phys.* **2010,** *132*, 154104.

12. Grimme, S.; Ehrlich, S.; Goerigk, L., Effect of the damping function in dispersion corrected density functional theory. *J. Comp. Chem.* **2011,** *32*, 1456-1465.

13. Hehre, W. J.; Ditchfie, R.; Pople, J. A., Self-Consistent Molecular Orbital Methods. 12. Further Extensions of Gaussian-Type Basis sets for use in molecular orbital studies of organic molecules. *J. Chem. Phys.* **1972,** *56*, 2257-2261.

14. Weigend, F.; Ahlrichs, R., Balanced basis sets of split valence, triple zeta valence and quadruple zeta valence quality for H to Rn: Design and assessment of accuracy. *Phys. Chem. Chem. Phys.* **2005,** *7*, 3297-3305.

15. Andrae, D.; Häußermann, U.; Dolg, M.; Stoll, H.; Preuß, H., Energy-adjusted ab initio pseudopotentials for the second and third row transition elements. *Theor. Chim. Acta* **1990,** *77*, 123-141.

16. Marenich, A. V.; Cramer, C. J.; Truhlar, D. G., Universal Solvation Model Based on Solute Electron Density and on a Continuum Model of the Solvent Defined by the Bulk Dielectric Constant and Atomic Surface Tensions. *J. Phys. Chem. B* **2009,** *113*, 6378-6396.

17. Neese, F., Software update: the ORCA program system, version 4.0. *Wiley Interdiscip. Rev. Comput. Mol. Sci.* **2017,** *8*, e1327.

18. Warren, J. J.; Tronic, T. A.; Mayer, J. M., Thermochemistry of Proton-Coupled Electron Transfer Reagents and its Implications. *Chem. Rev.* **2010,** *110*, 6961-7001.